Amplified summer warming in Europe-West Asia and Northeast Asia after the mid-1990s

Riyu Lu, Xiaowei Hong, and Shuanglin Li
Institute of Atmospheric Physics, Chinese Academy of Sciences, Beijing 100029, China

2017-08-01，ITCP-TTA

Contents

- Importance of temperature impact
- Regional feature of warming
- Possible reason for regional warming
- Summary

Keeling curve: CO2 increasing

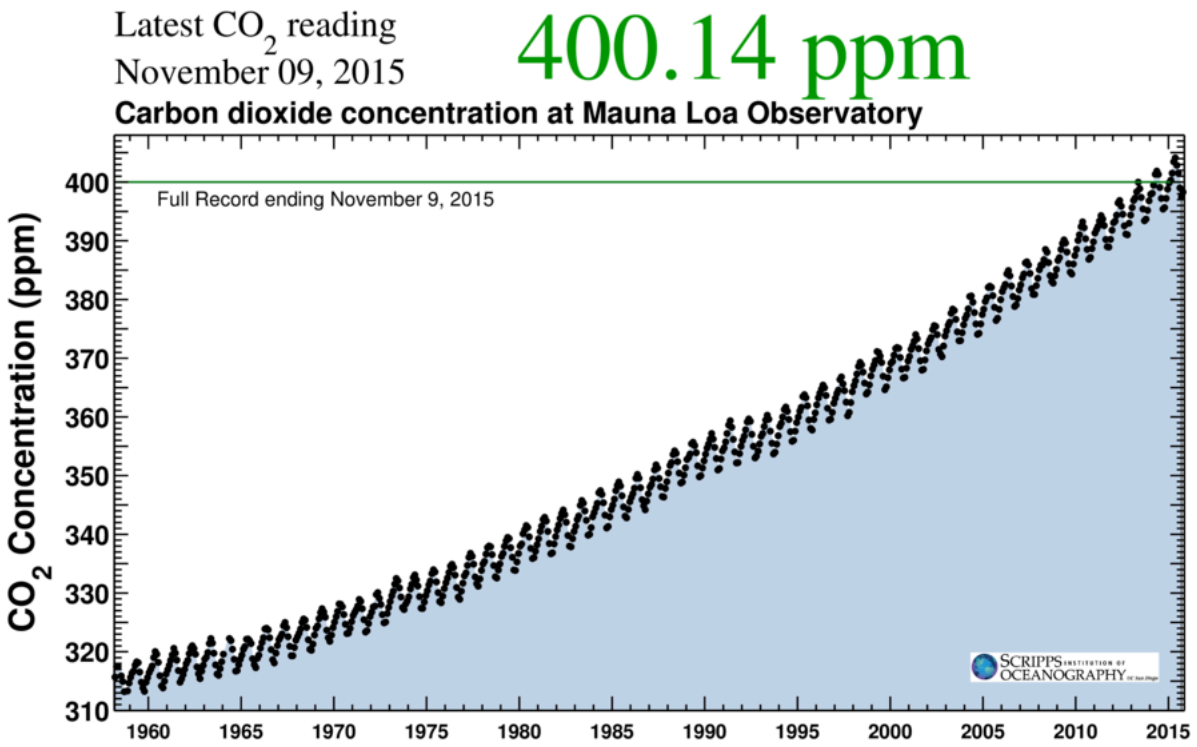

Global warming, Regional warming

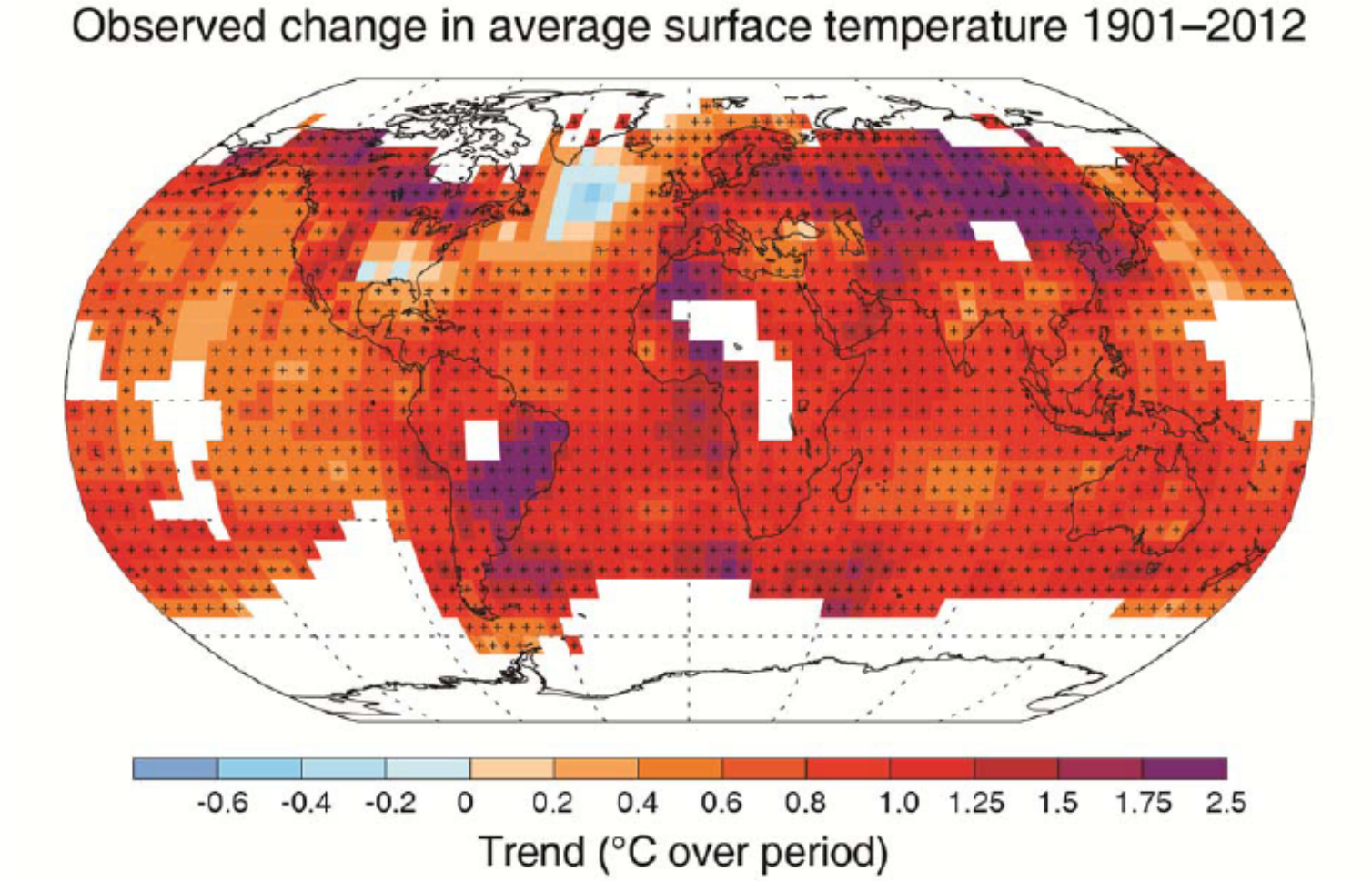

IPCC AR5 WG1 SPM 2013

EXTREME HEAT EVENTS WILL BECOME MORE SEVERE

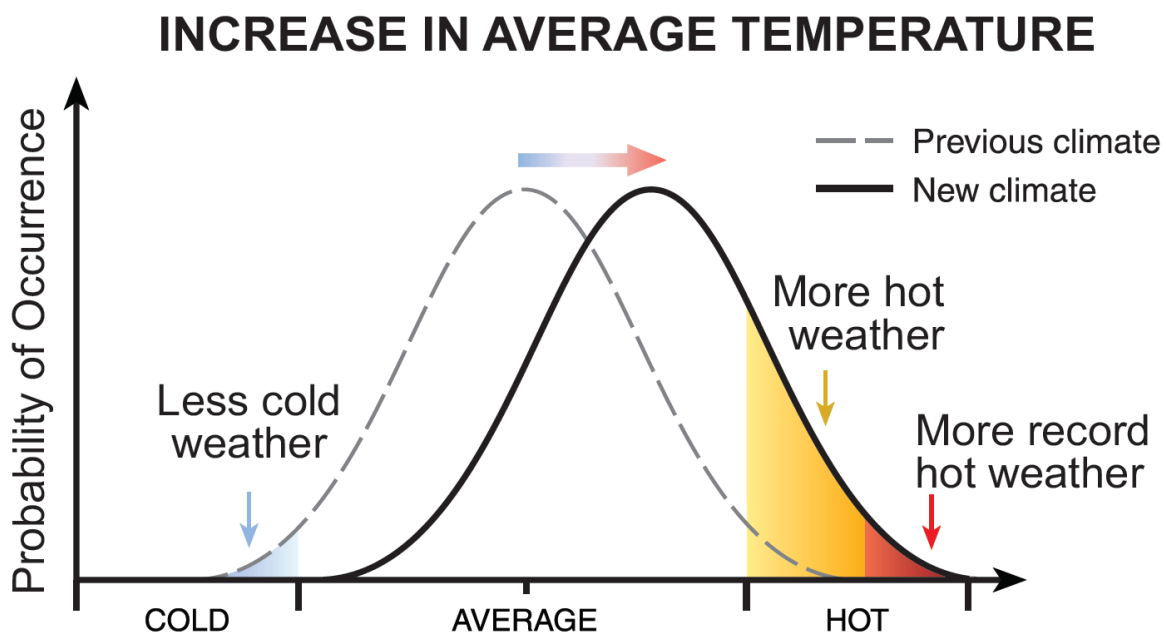

When average temperatures increase, the average temperature of "hot weather" and "record hot weather" will become even hotter.[16]

From CDC

Casualties increasing dramatically

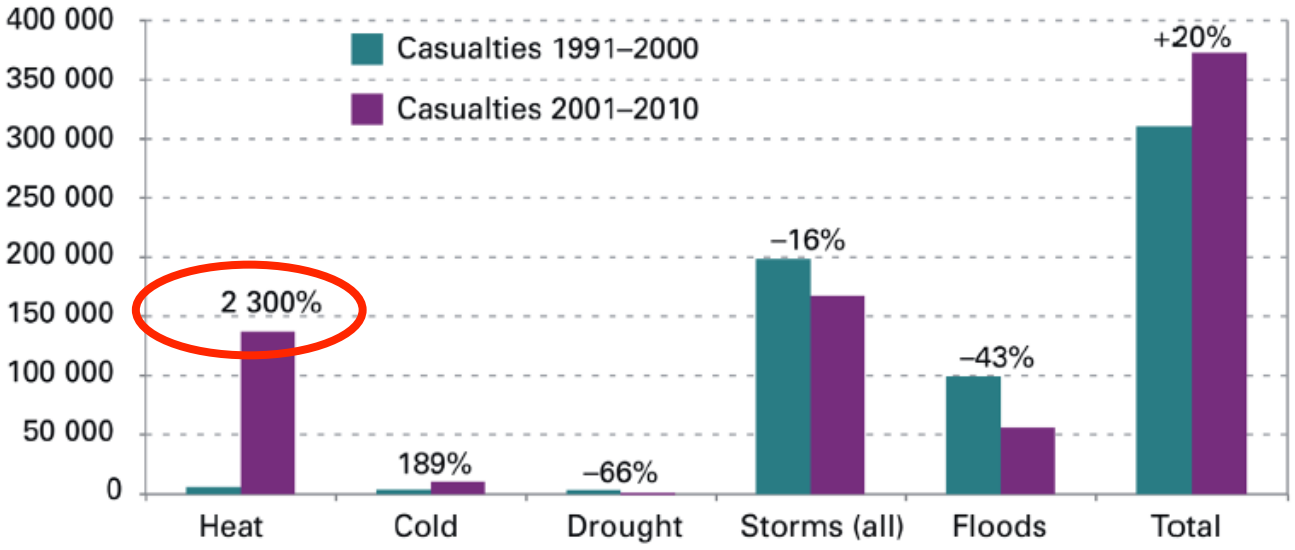

(World Meteorological Organization 2013)

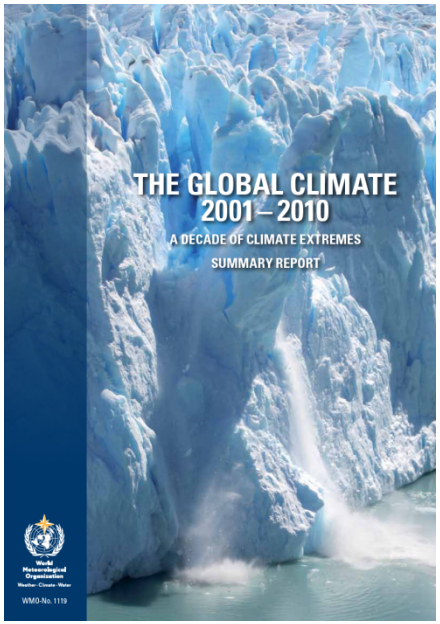

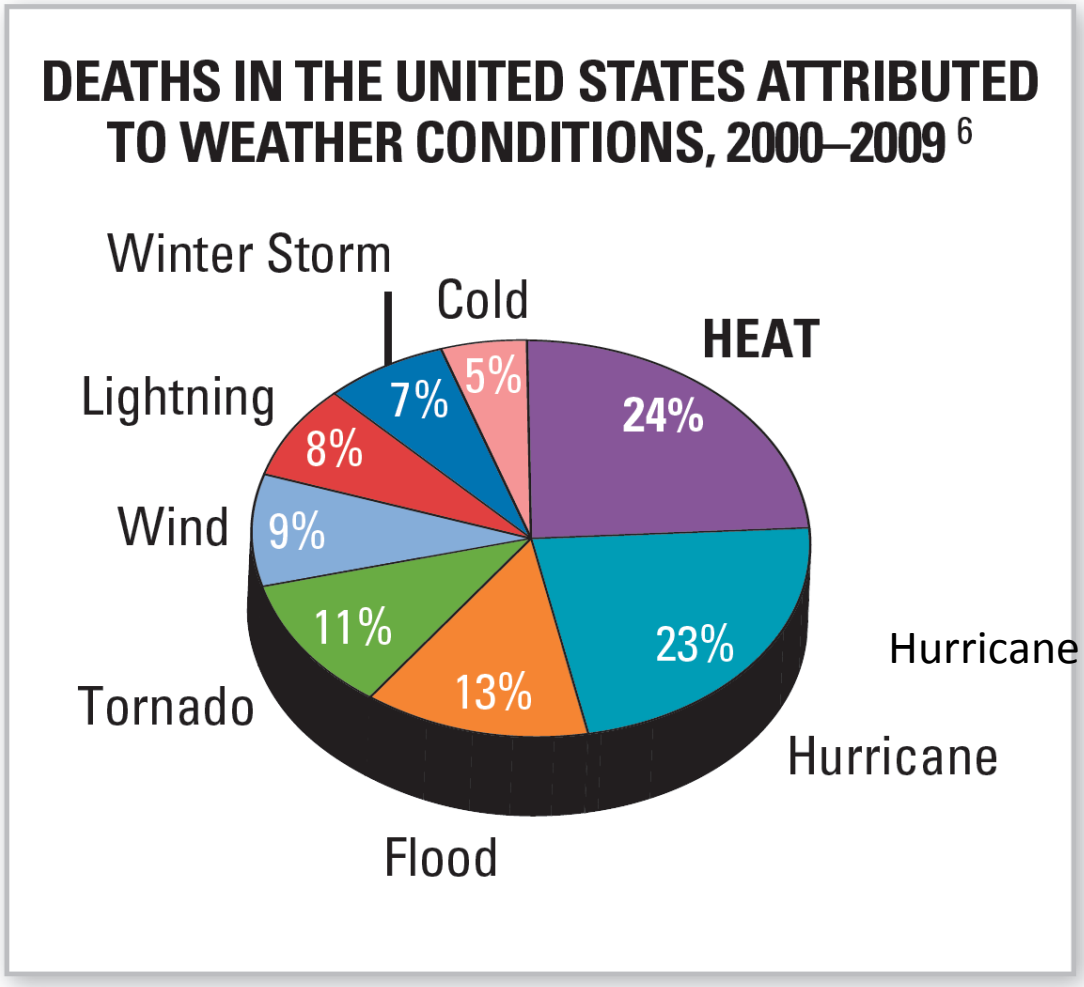

Hurricane Katrina, August 2005

From CDC, USA

Centers for Disease Control and Prevention
Communicable Disease Center

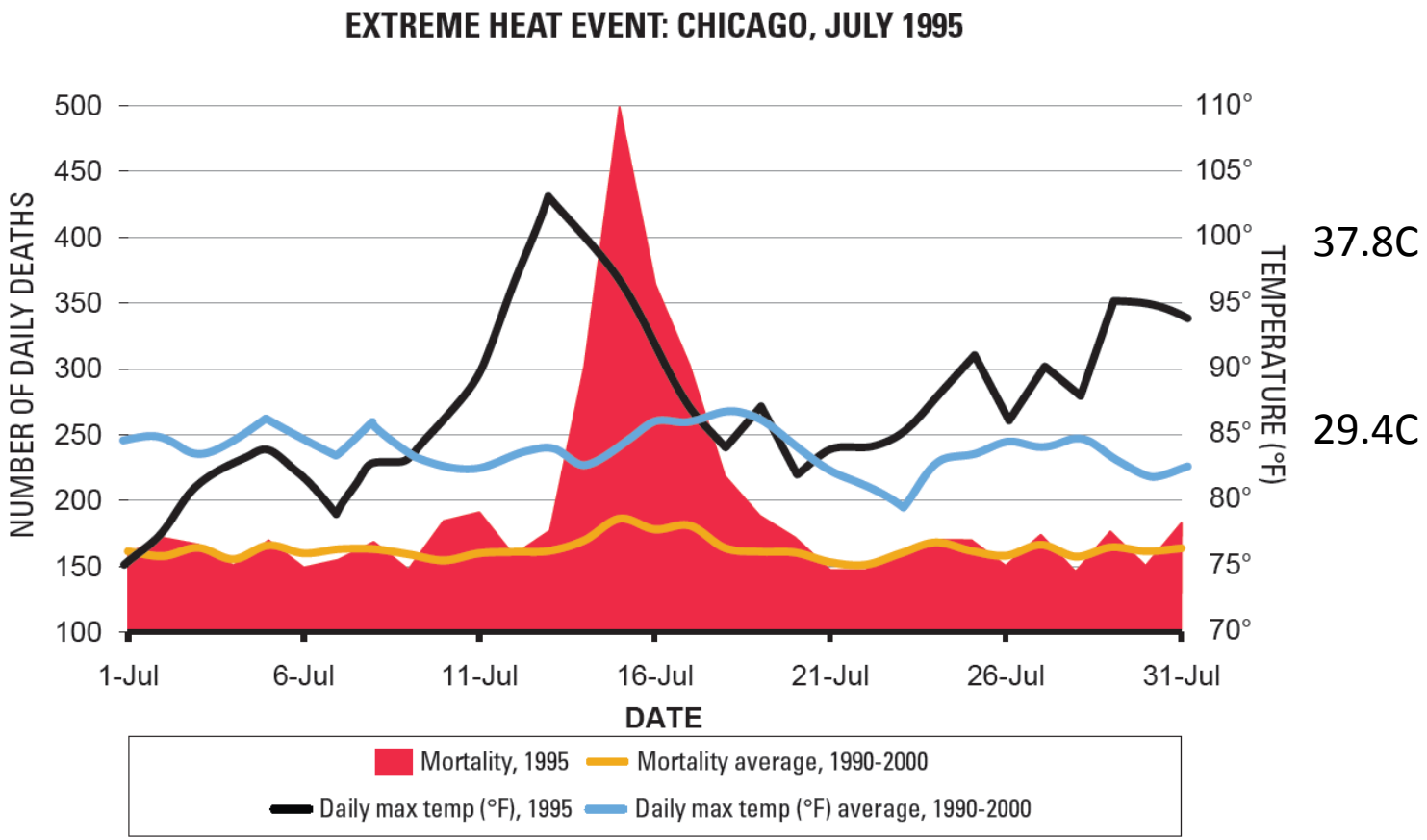

37.8C

29.4C

One of the most severe extreme heat events in recent U.S. history occurred in July 1995 in Chicago. During this event, the extended increase in daily maximum temperatures (black line) as compared to the average for 1990-2000 (blue line) had an estimated result of more than 650 deaths.[3]

From CDC

Although warming brings great challenges, there may be some be benefits from it.

Northeast China: Important Base of Grain Production

1/5 of total production in China

Cultivated land area increases greatly in Northeast China

	1990	2010	%
Cultivated area	1623	2149	**32.4%**

(unit: hm2, hectare)

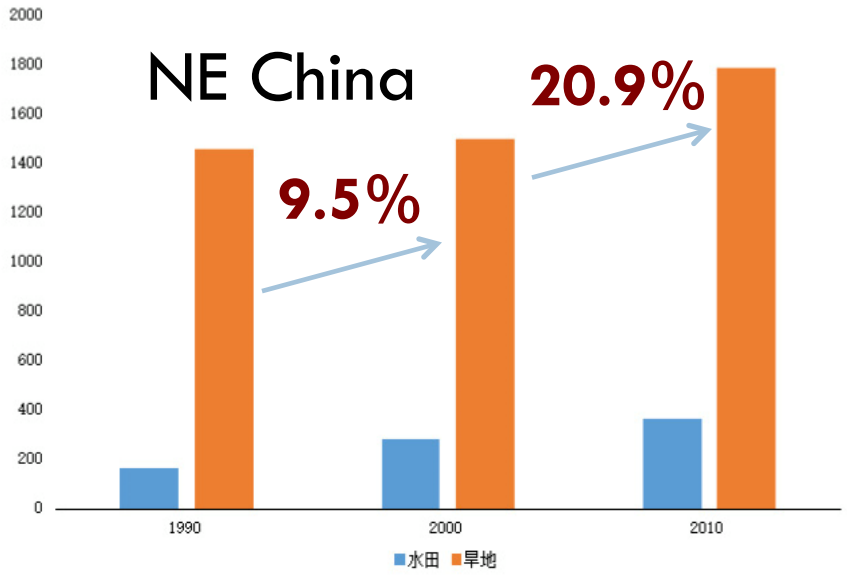

Why the cultivated area increasing in Northeast China:

- China needs more crop product
- China's policy
- More high-tech used
- … …

Possible reason for more cultivated area in Northeast China

Northeast Asia experienced an extraordinary warming trend

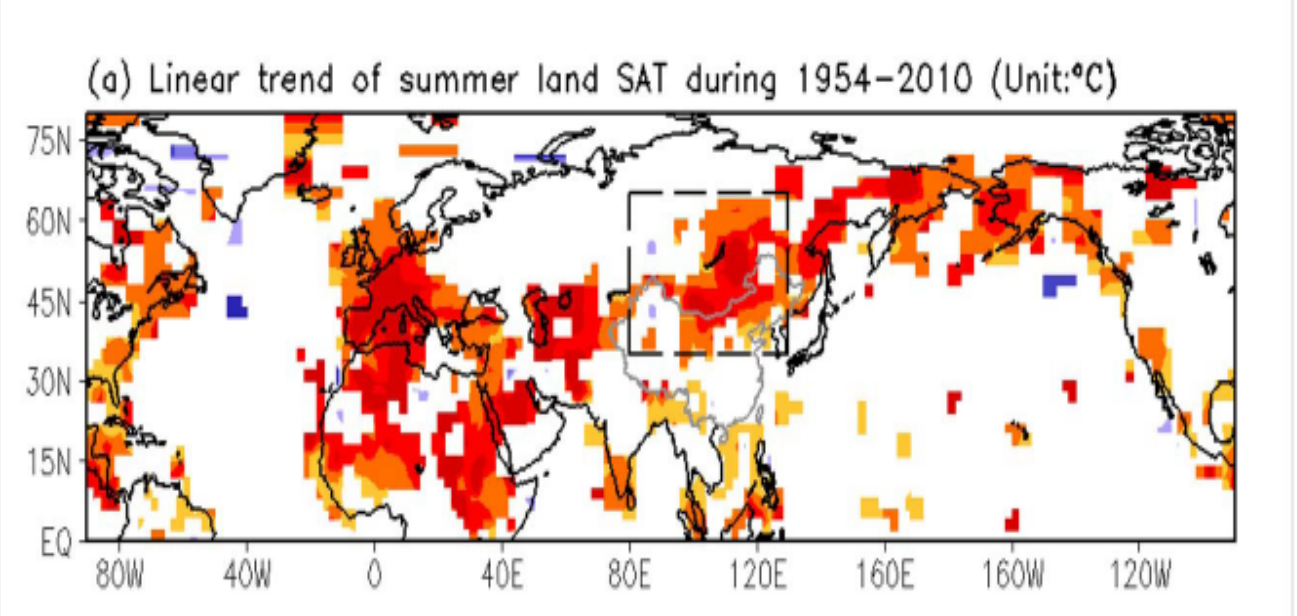

Zhu et al. *(2012) GRL*♪

Became warmer particularly since middle 1990s

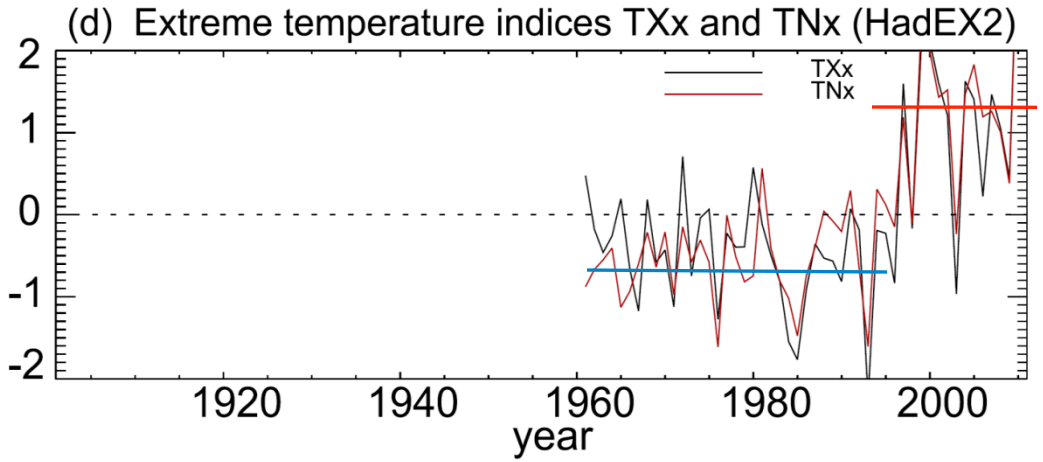

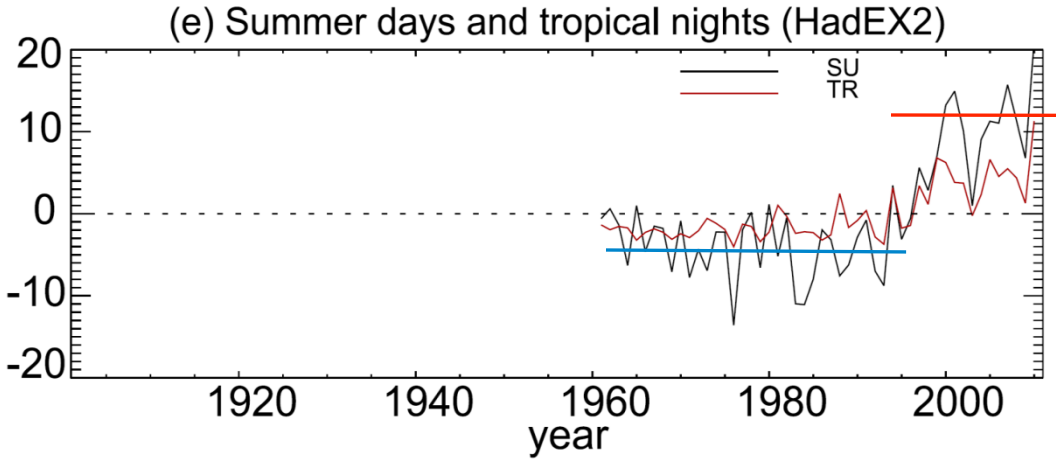

Both maximum and minimum temperature increases

Summer becomes longer ~15 days

Summer day: Tmax>25C

Tropical Night: Tmin>25C

Temperature increase since mid-1990s, particularly over Europe and Northeast Asia

(*Sutton and Dong*, 2012; *Stainforth et al*., 2013; *Chen and Lu*, 2014; *Dong et al*., 2016; *Dong et al*., 2017)

P1: 1964-1996

P2: 1997-2016

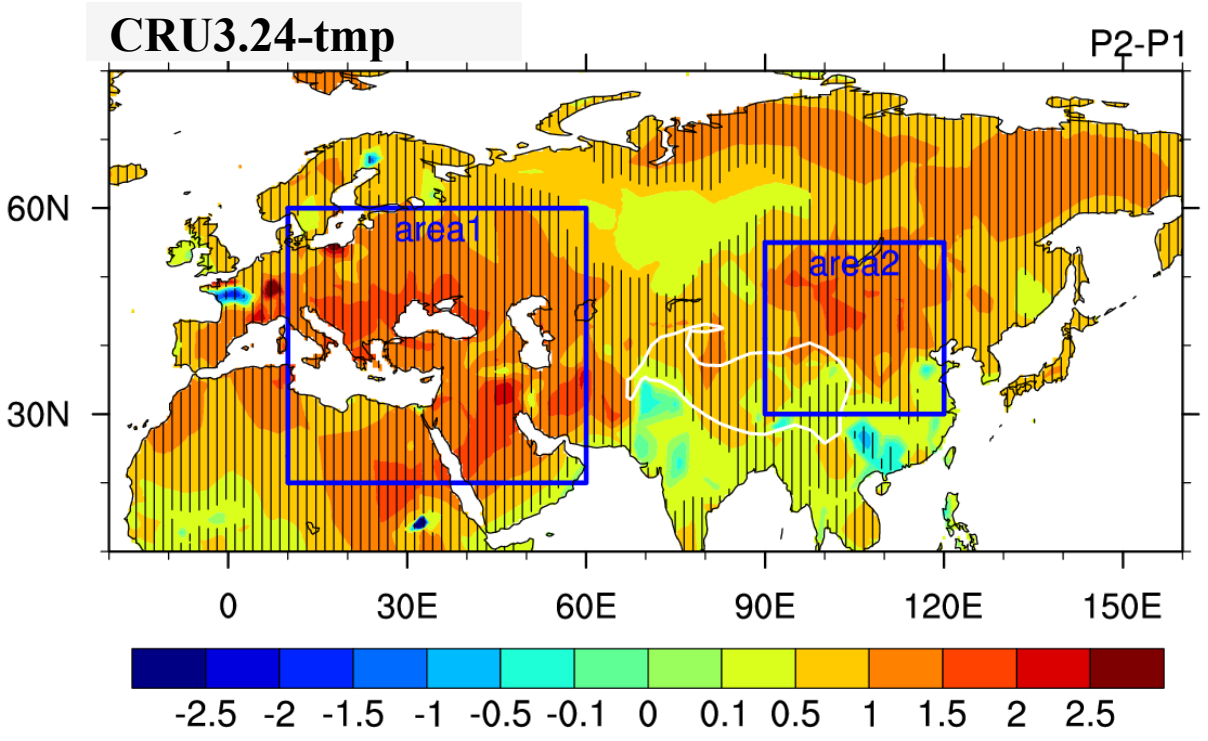

Possible mechanism for regional warming

- Polar amplification: temperature increases more quickly in high latitudes of the northern hemisphere (Screen and Simmonds 2010, 32 Pithan and Mauritsen 2014, Xie *et al 2015).*
- Land warming greater than ocean warming (Sutton et al 2007, Dong et al 2009, Boer 2011, Joshi et al 2013).
- Drier land warming greater than wetter land warming (Zhou et al 2015, 2016).

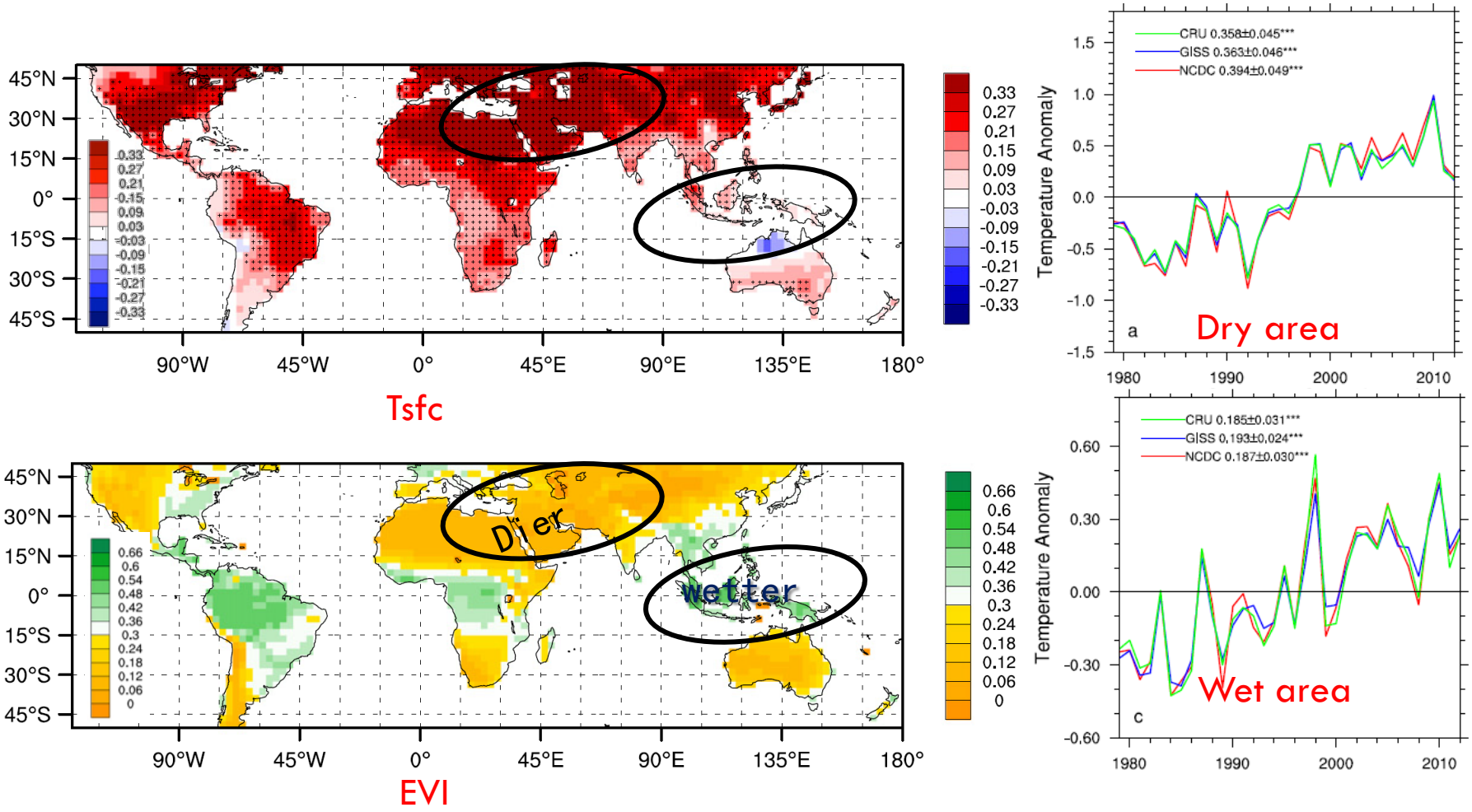

Zhou L., H. Chen, W. Hua, Y. Dai, N. Wei. **2016** Mechanisms for stronger warming amplification over drier ecoregions observed since 1979. **Clim. Dyn.**, 47(9-10):2955-2974.

Zhou L., H. Chen, Y. Dai. **2015** Stronger warming amplification effects over drier ecoregions observed since 1979. **Environ. Res. Lett.**, 10 (6): 064012. doi:10.1088/1748-9326/10/6/064012.

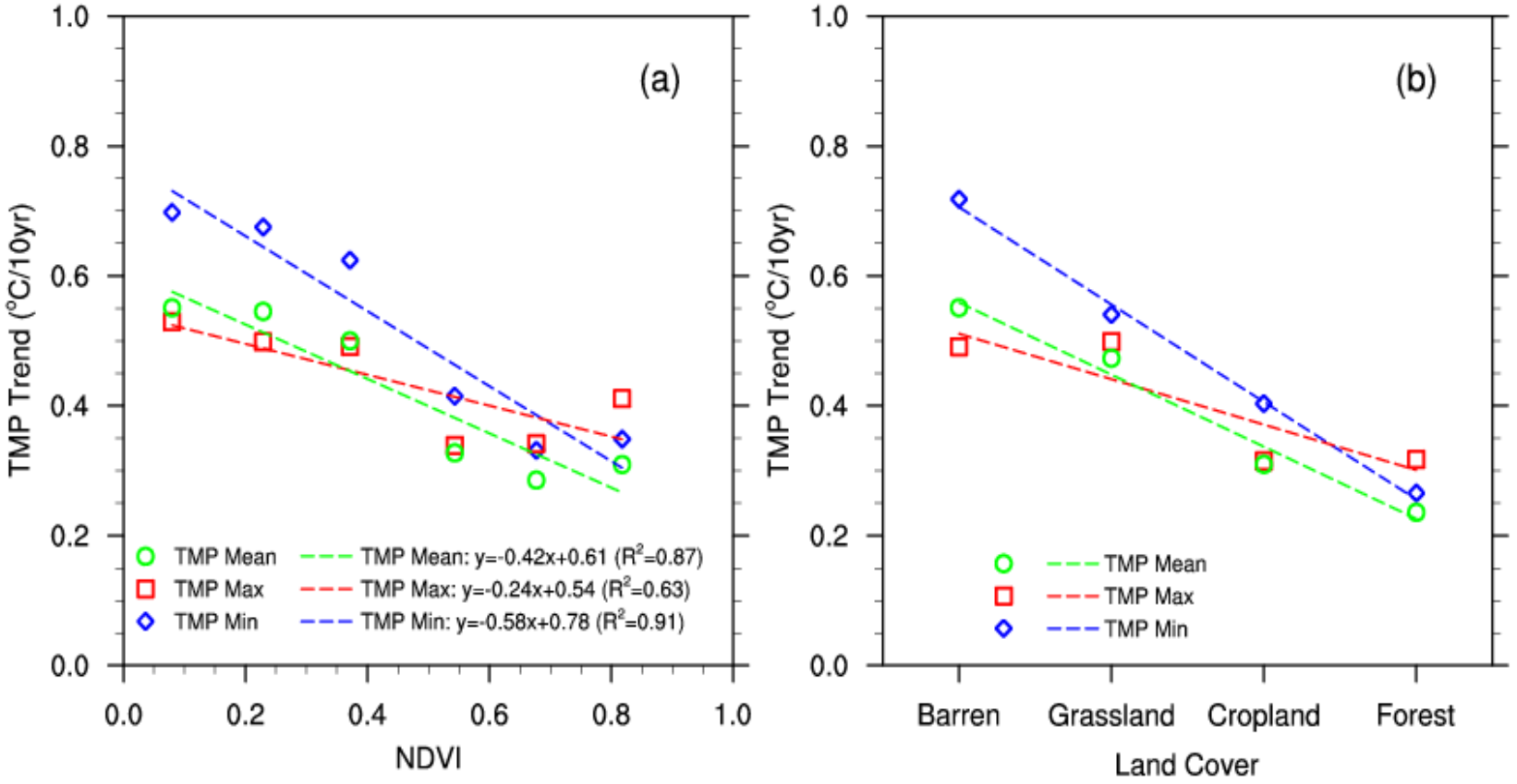
(a)
TMP Trend (°C/10yr)
NDVI
1.0
0.8
0.6
0.4
0.2
0.0
0.0
0.2
0.4
0.6
0.8
1.0
TMP Mean
TMP Max
TMP Min
TMP Mean: y=-0.42x+0.61 (R2=0.87)
TMP Max: y=-0.24x+0.54 (R2=0.63)
TMP Min: y=-0.58x+0.78 (R2=0.91)
(b)
TMP Trend (°C/10yr)
Barren
Grassland
Cropland
Forest
Land Cover
TMP Mean
TMP Max
TMP Min

Possible mechanism for regional warming

- Polar amplification: temperature increases more quickly in high latitudes of the northern hemisphere.
- Land warming greater than ocean warming
- Drier land warming greater than wetter land warming

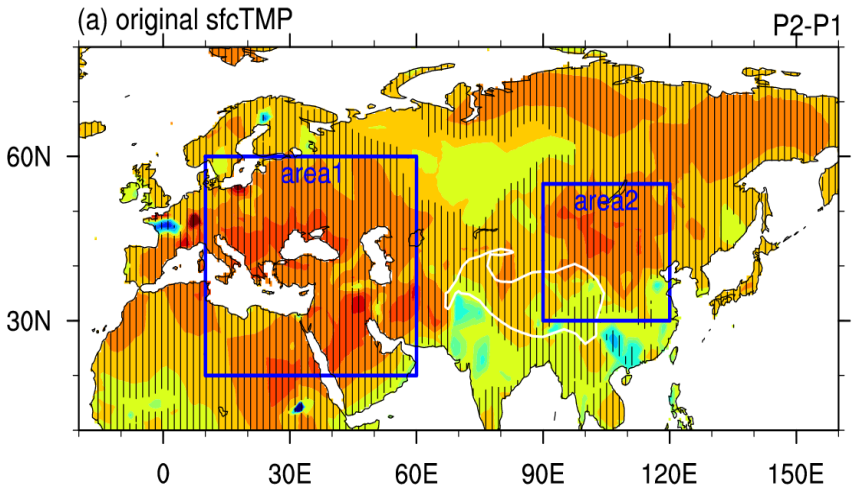

Natural process

High pressure

→Down flow
→Less cloud
→More solar radiation

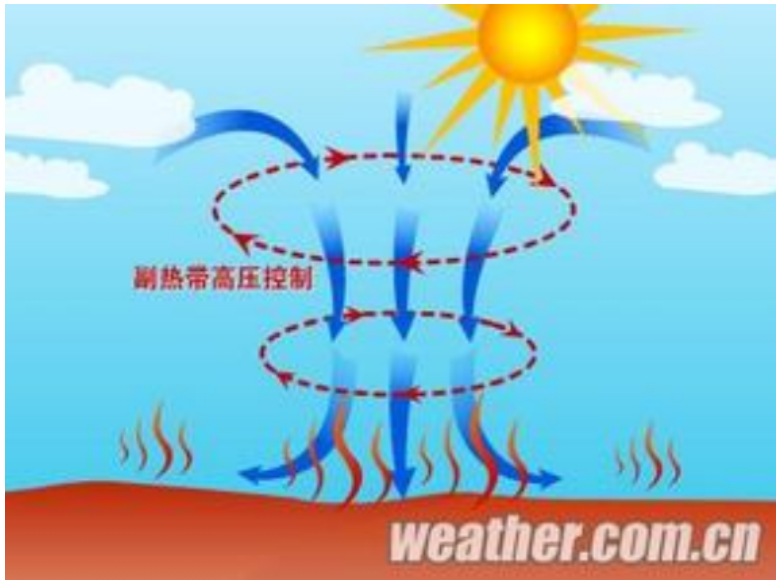

High temperature

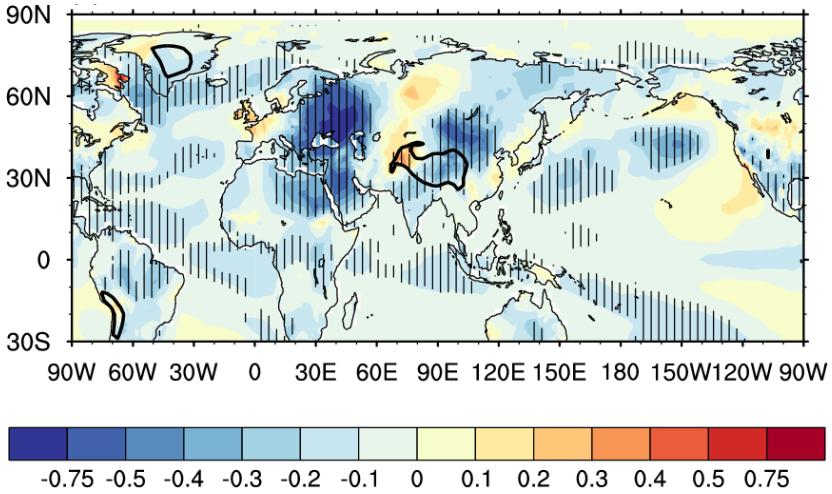

Silk Road Pattern-related temperature

The regional feature of Eurasian warming is similar to the temperature anomalies associated with the Silk Road Pattern

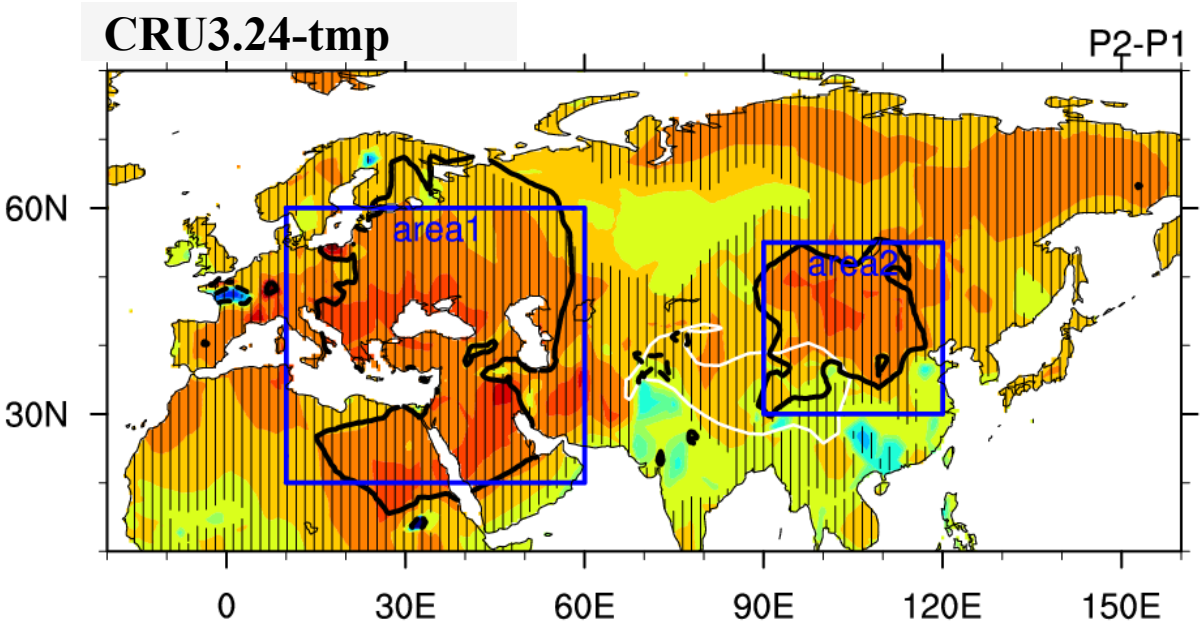

Black bold lines represent the areas of Silk Road Pattern-related temperature

Silk Road Pattern A teleconnection along the jet

Teleconnection along the jet

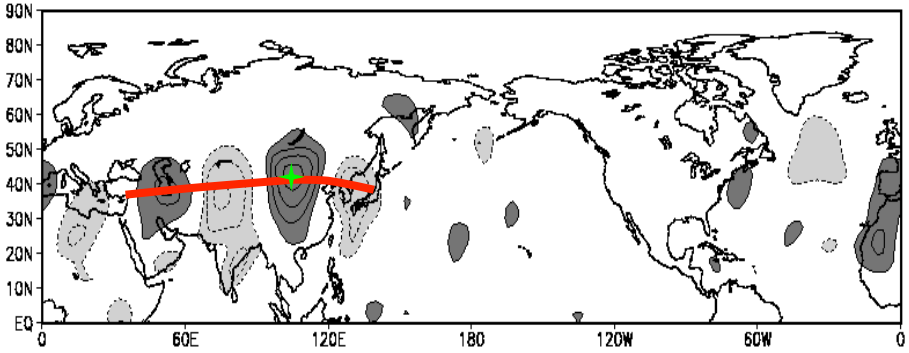

(Lu et al. 2002)

Circumglobal Teleconnection

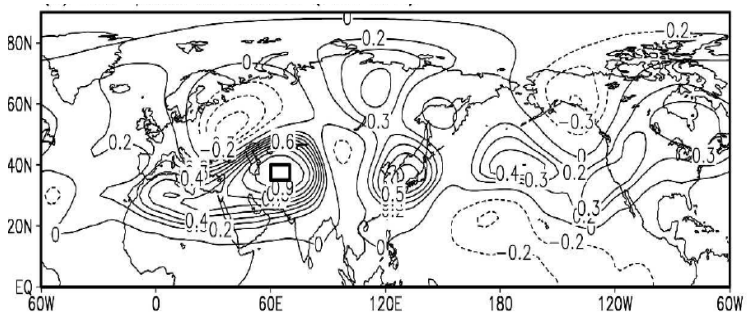

(Ding and Wang, 2005)

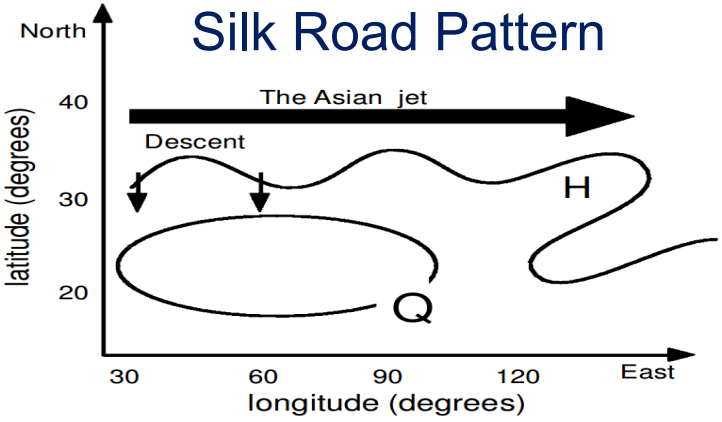

(Enomoto et al., 2003)

EOF-V200

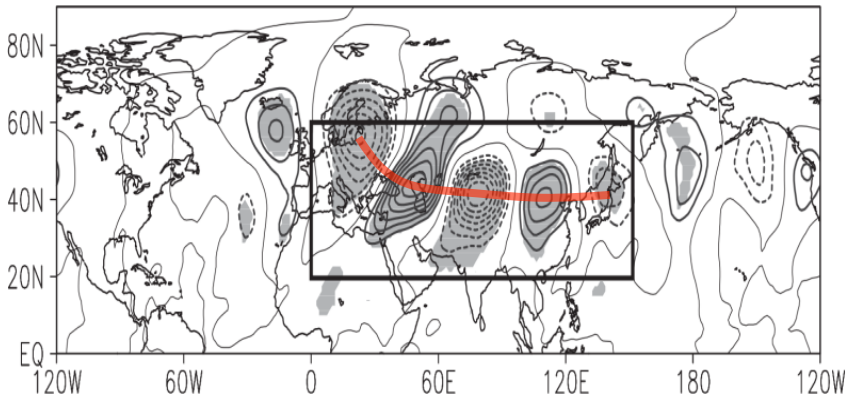

(Sato and Takahashi, 2006; Yasui and Watanabe, 2010)

Summer Asian Jet

200-hPa zonal wind

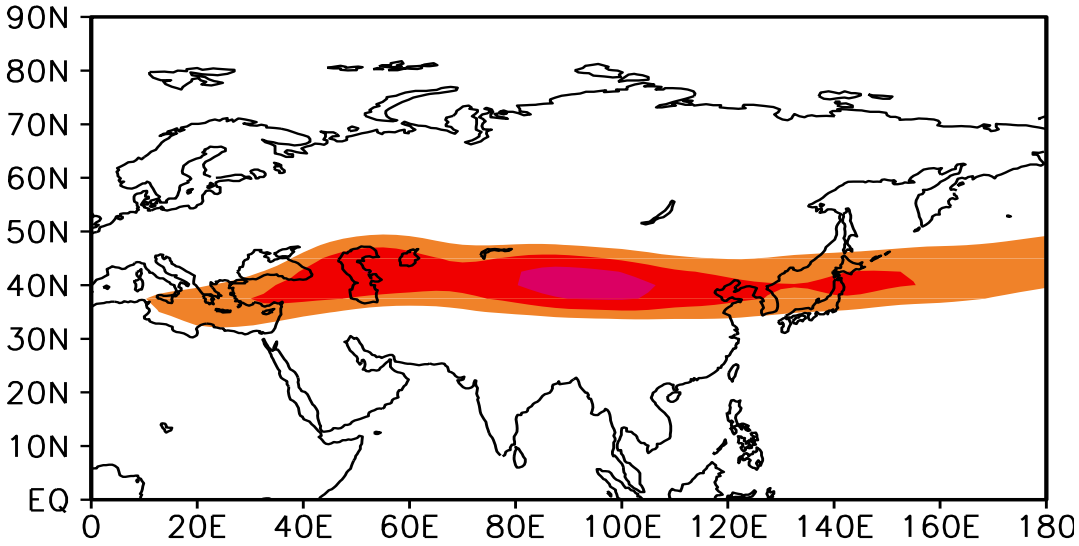

Upper-tropospheric jet

U200: 20-40m/s

Theory of jet waveguide

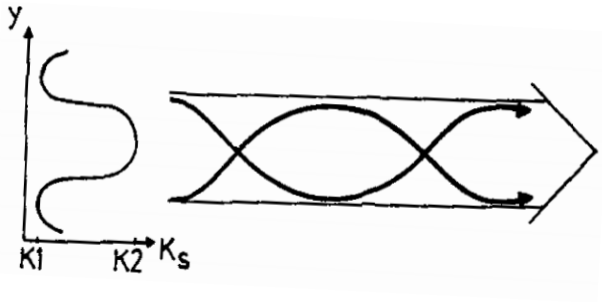

(Hoskins & Ambrizzi, 1993)

strong westerly jet acts as the waveguide and confines the waves within it

Wavelength is determined by basic flows

Ks≈6， wavelength is ~60 degrees

$$K_s = \left(\frac{a\beta_M}{\bar{v}}\right)^{1/2}$$
$$= \left\{\left[2\Omega - \left(\frac{1}{\cos\phi}\frac{\partial}{\partial\phi}\right)^2(\cos^2\phi\bar{v})\right]\Big/\bar{v}\right\}^{1/2}\cos\phi$$

(Hoskins and Ambrizzi, 1993)

SRP affects the northern hemisphere climate

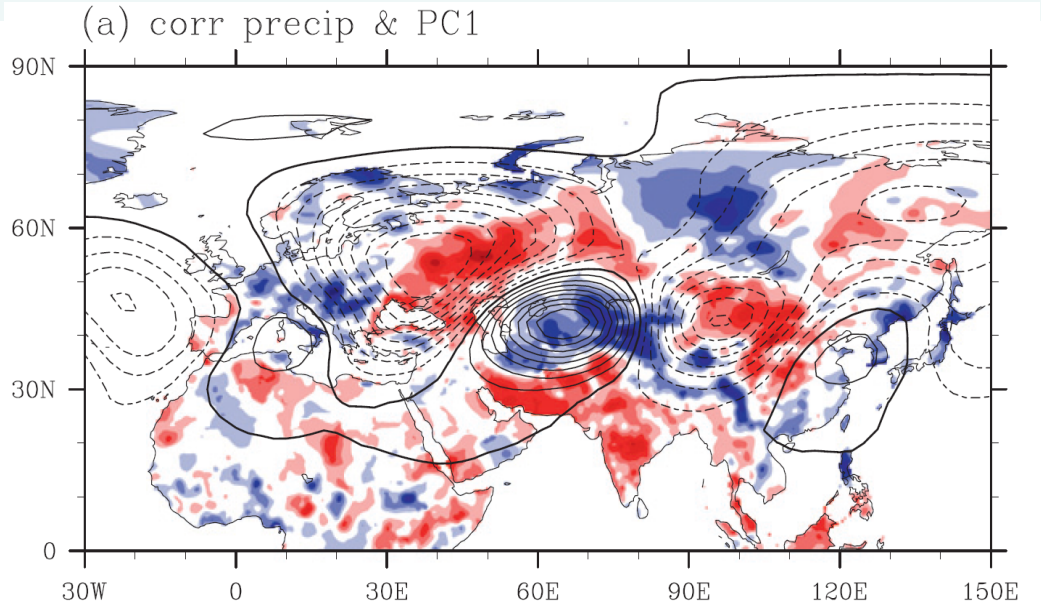

Chen and Huang 2012

✓Surface air temperatures (Enomoto 2004; Wakabayashi and Kawamura 2004; Ding and Wang 2005; Sato and Takahashi 2006; Ding et al. 2011; Zhang and Jin 2016)

✓Rainfall (Lu et al. 2002; Tao and Wei 2006; Huang et al 2011; Chen and Huang 2012;Ding et al. 2013; Saeed et al. 2014; Su and Lu 2014; Zhang and Jin 2016)

✓……

Index definition

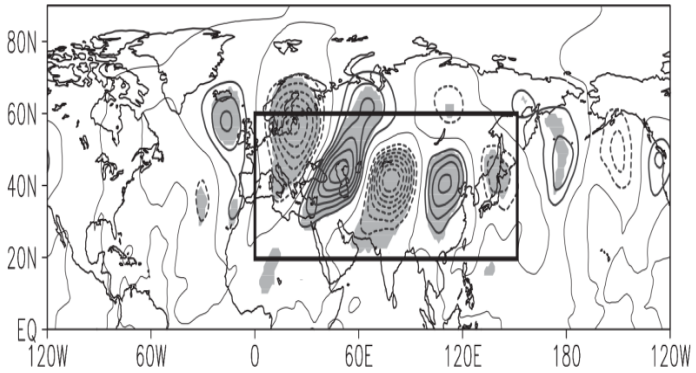

(Yasui and Watanabe 2010)

Silk Road Pattern (SRPI)

Normalized PC1 of the V200-EOF within (20º-60ºN, 0º-150ºE)

SRPI＞0, a positive phase SRP

Silk Road Pattern

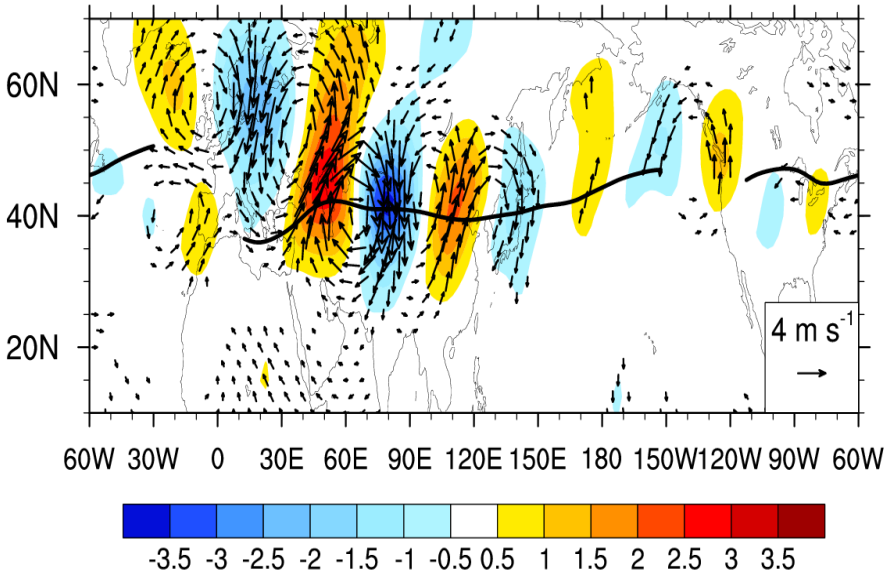

SRPI shows a strong decadal change, explaining 29.6% of total variance.

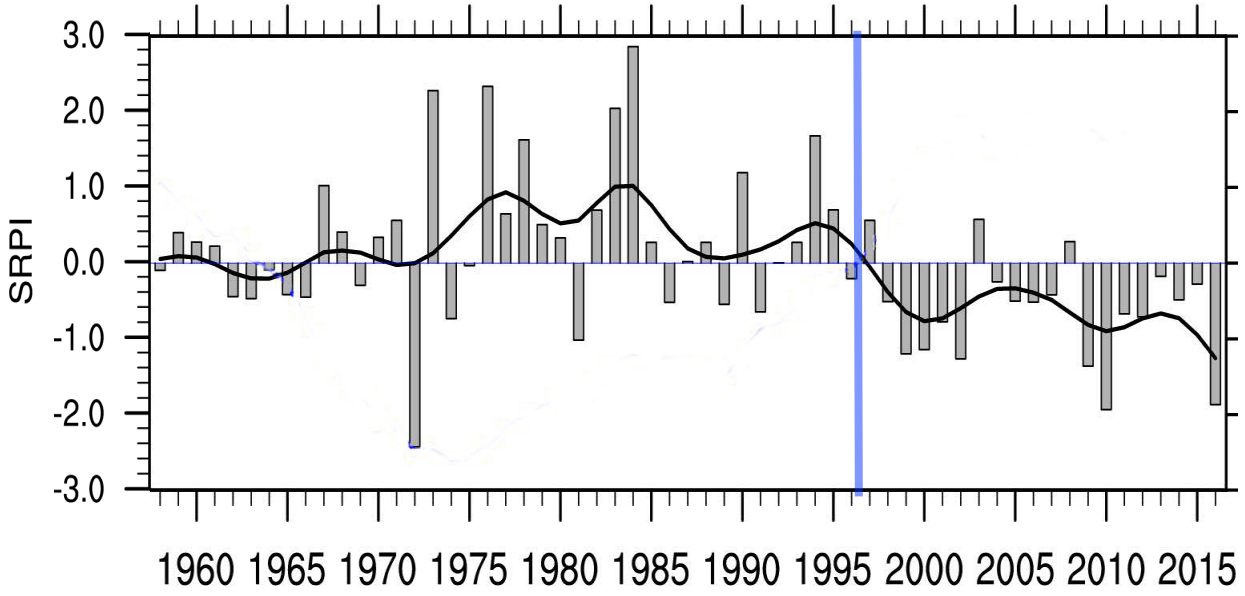

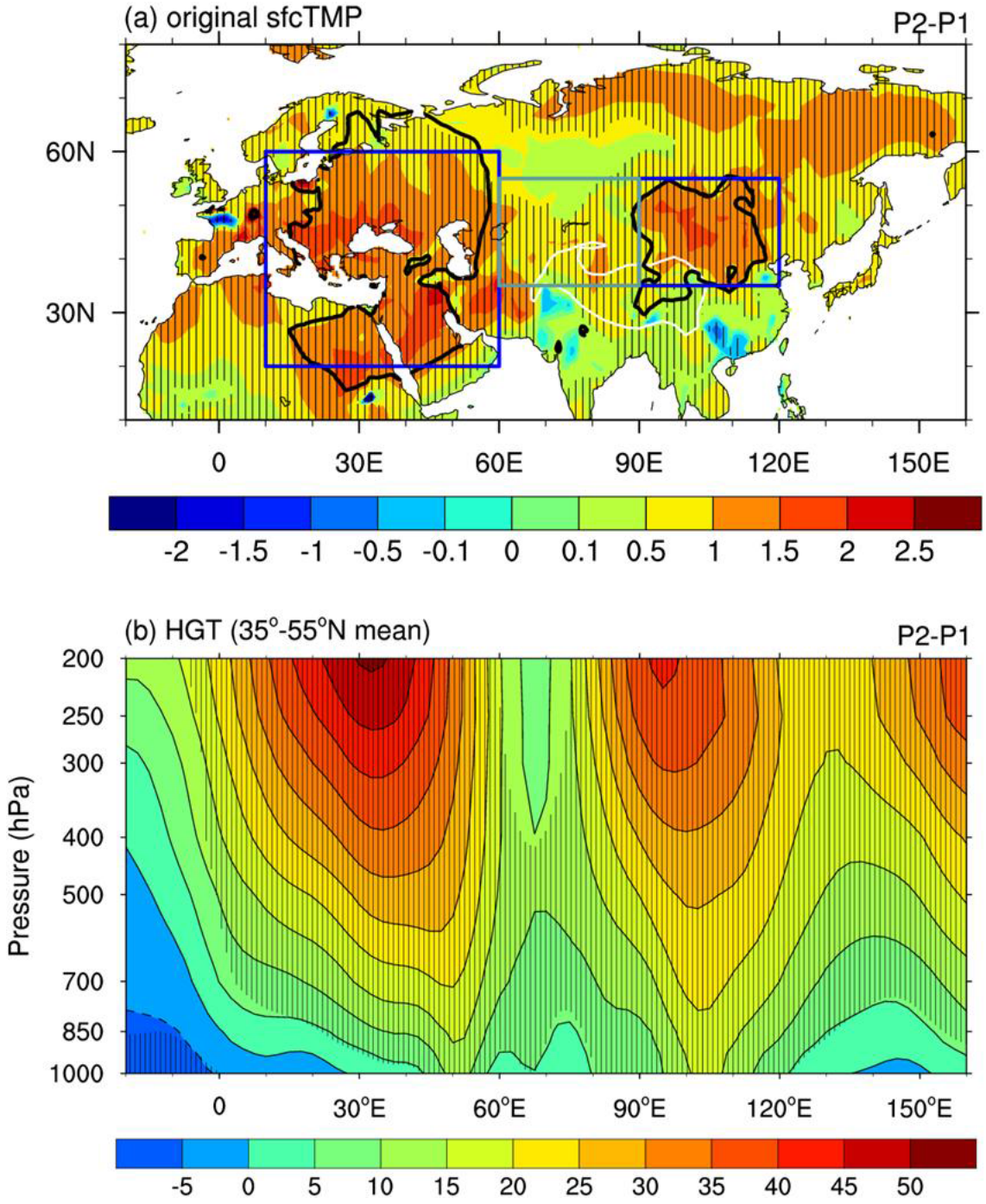
(a) original sfcTMP
P2-P1
60N
30N
0
30E
60E
90E
120E
150E
-2
-1.5
-1
-0.5
-0.1
0
0.1
0.5
1
1.5
2
2.5
(b) HGT (35°-55°N mean)
P2-P1
Pressure (hPa)
200
250
300
400
500
700
850
1000
0
30°E
60°E
90°E
120°E
150°E
-5
0
5
10
15
20
25
30
35
40
45
50

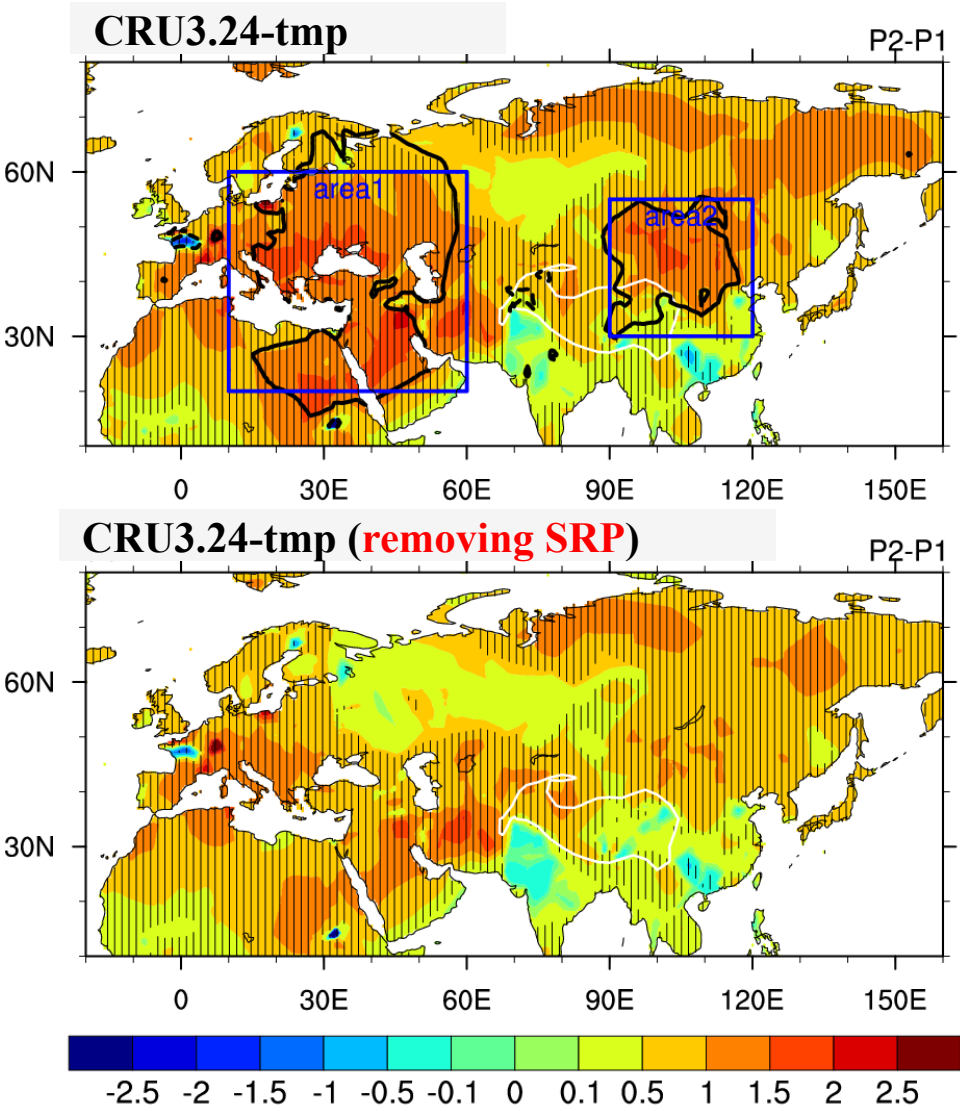

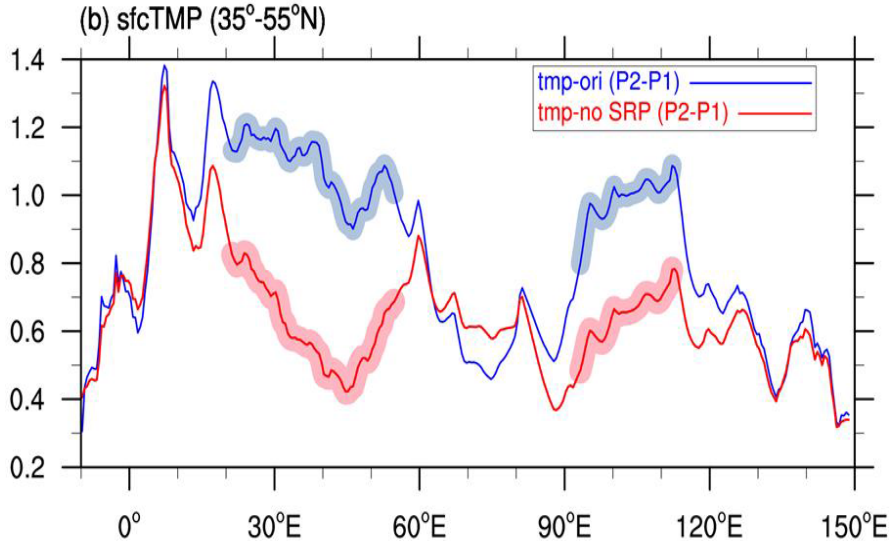

After removing SRP, the warming tends to be uniform.

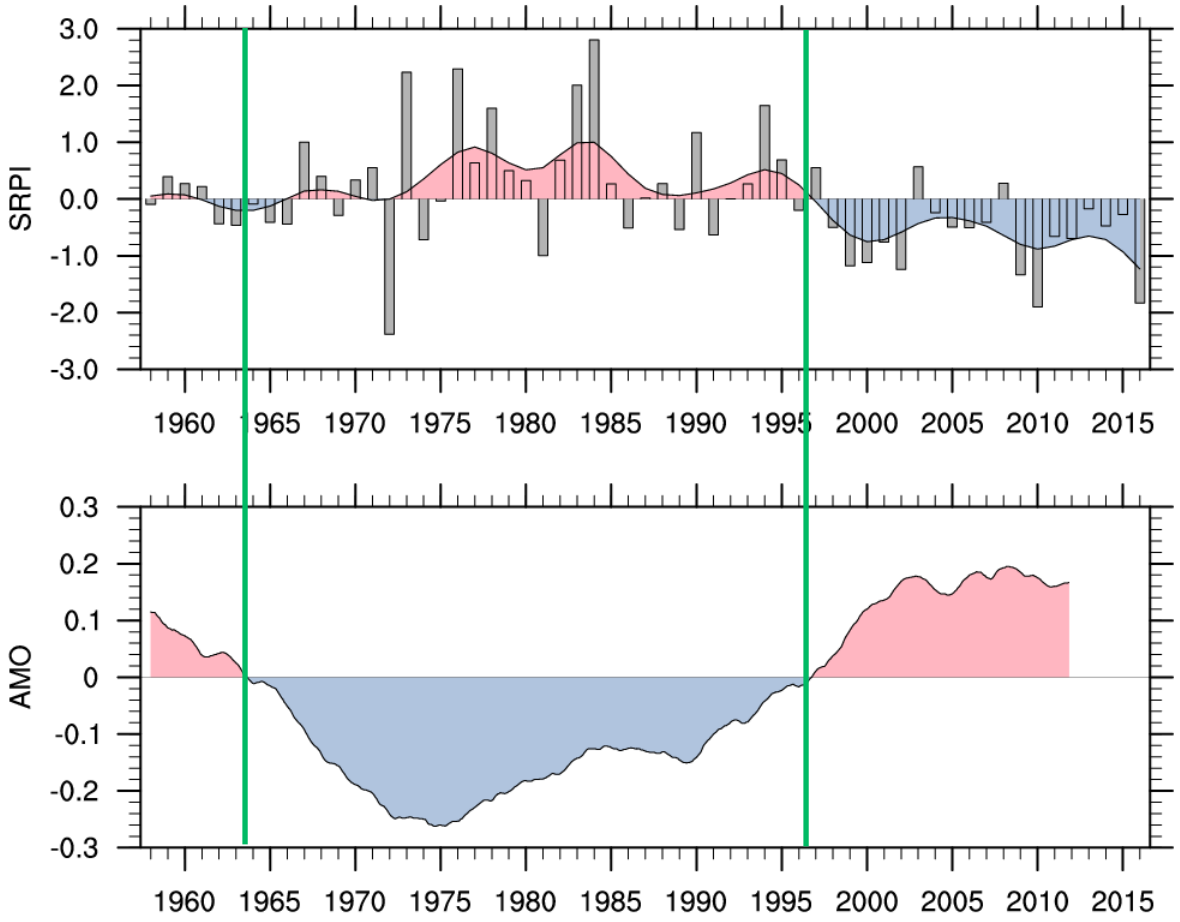

Silk Road Pattern

AMO

AMO concurs with the decadal change in SRP

AMO: Atlantic Multidecadal Oscillation

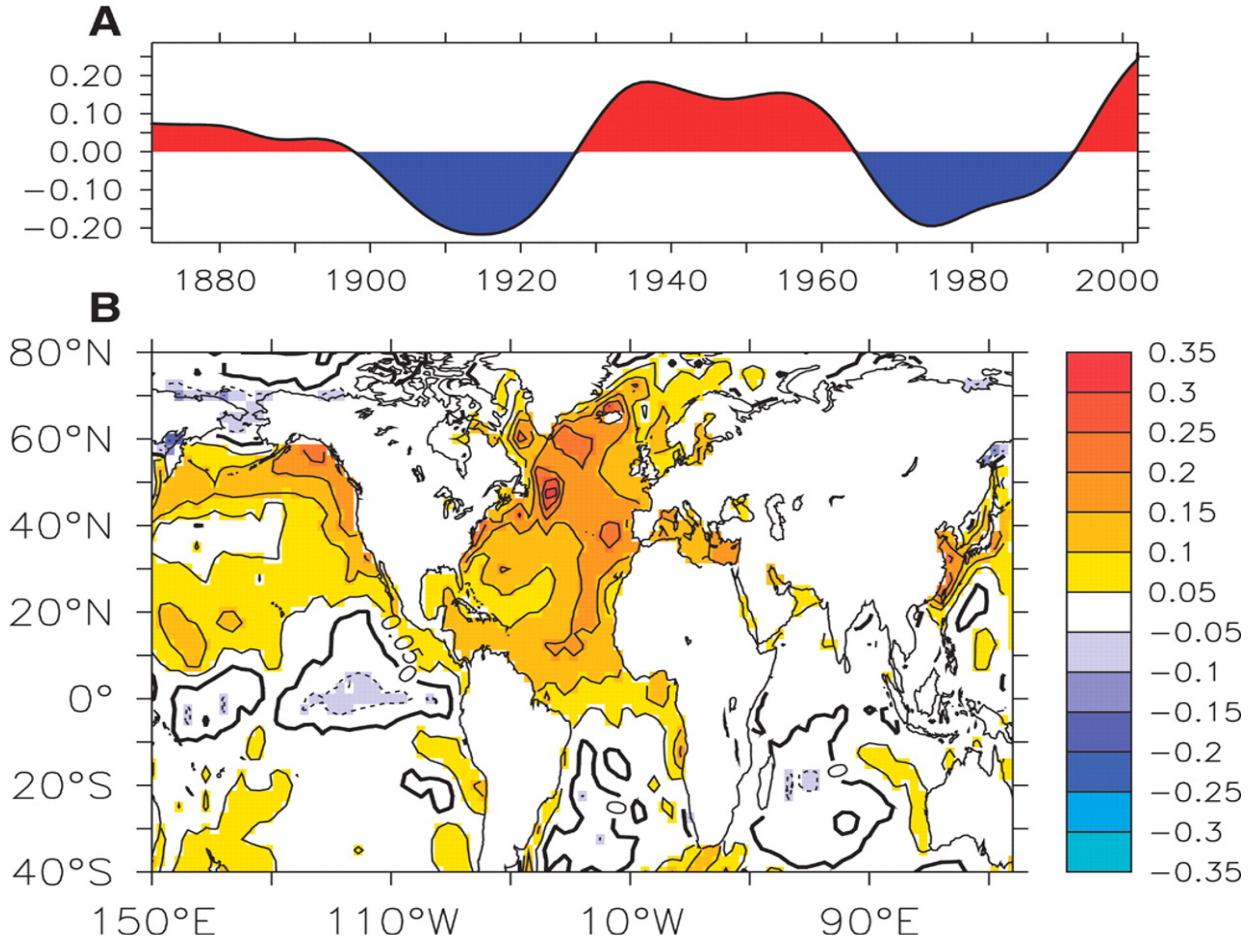

From Sutton et al. *Science* 2005

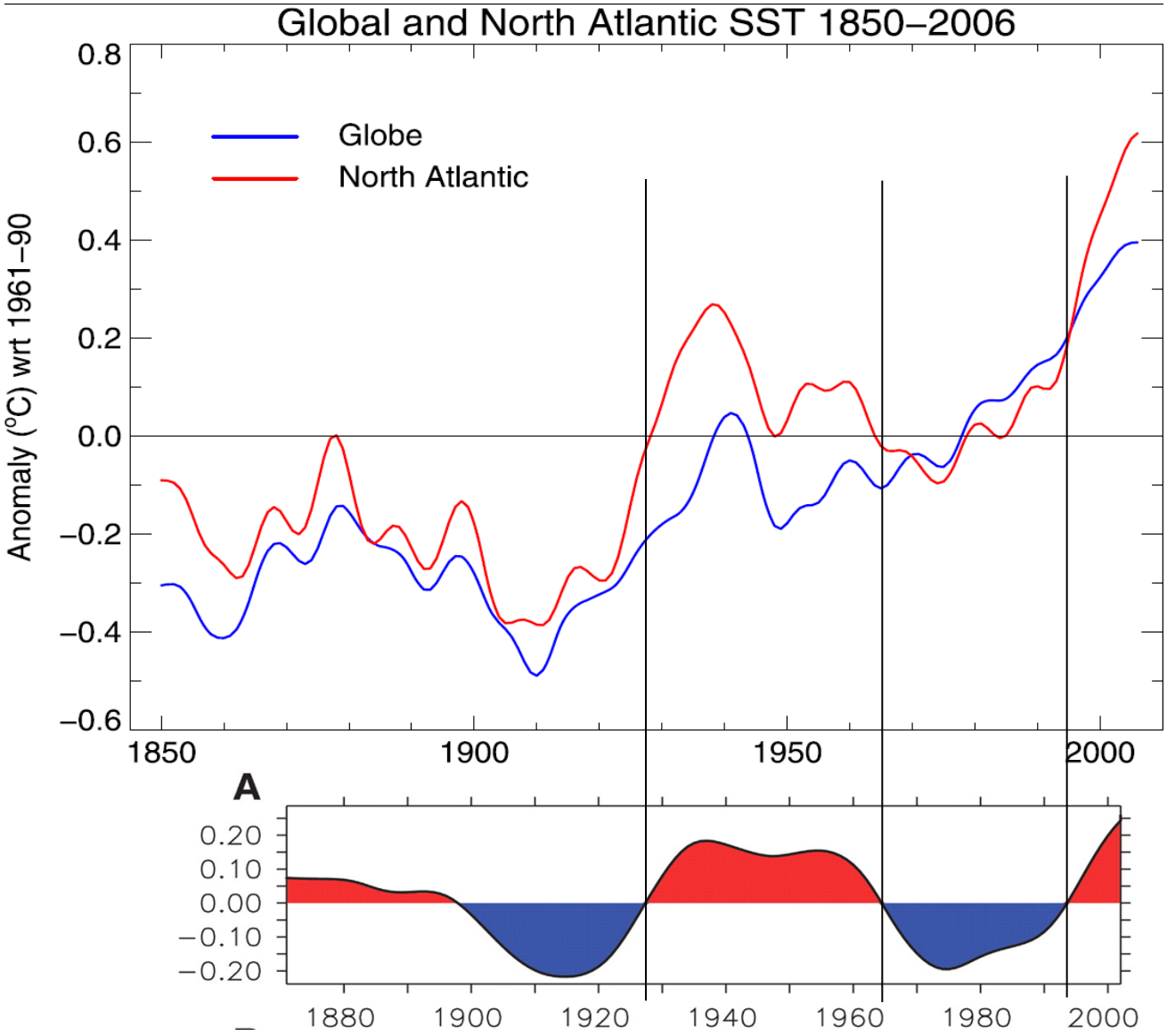
Global and North Atlantic SST 1850–2006
Globe
North Atlantic
Anomaly (°C) wrt 1961–90
0.8
0.6
0.4
0.2
0.0
−0.2
−0.4
−0.6
1850
1900
1950
2000
A
0.20
0.10
0.00
−0.10
−0.20
1880
1900
1920
1940
1960
1980
2000

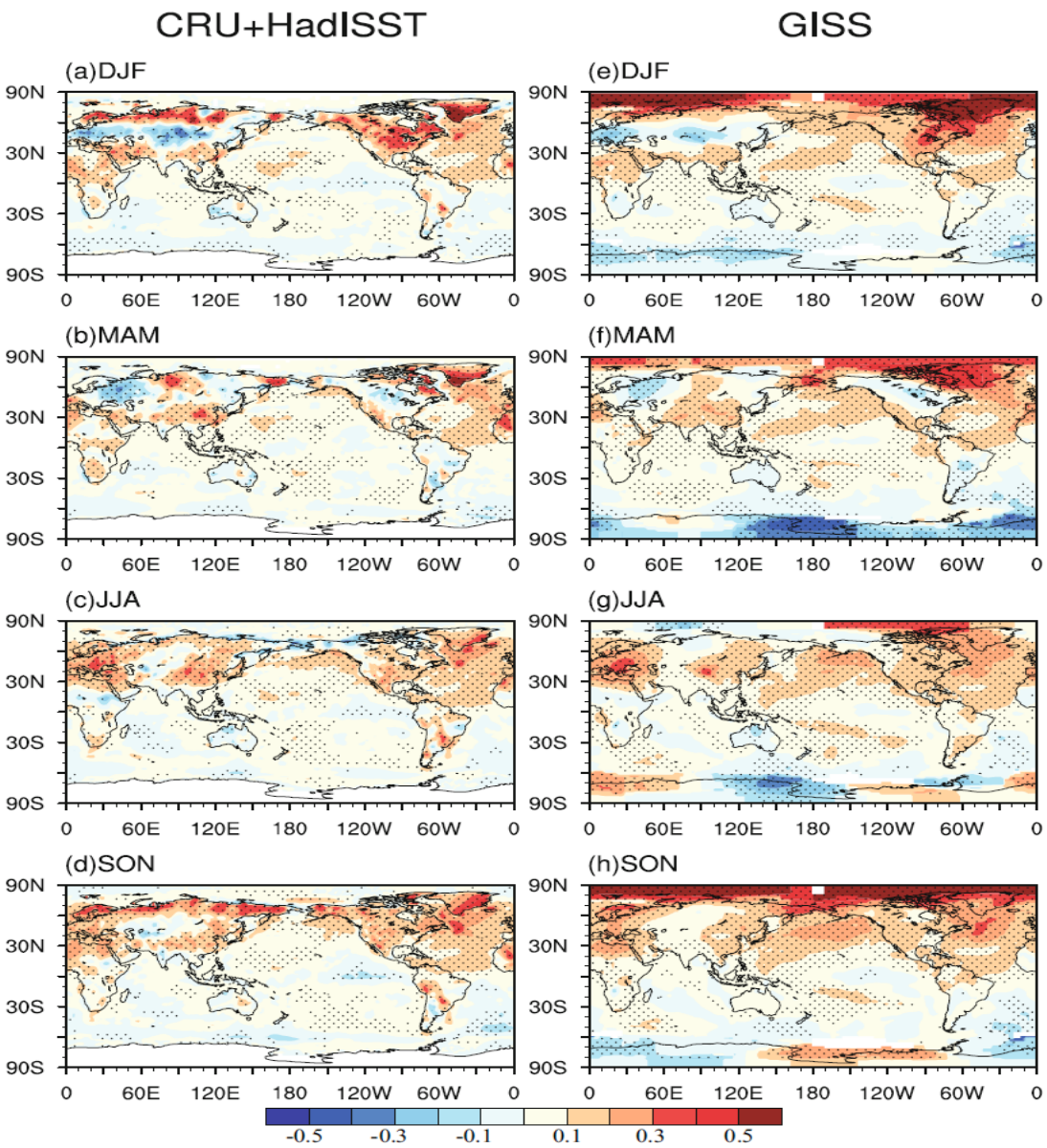

Fig. 7. Regressions of surface temperature onto the standardized AMO index: (a–d) CRU (for land temperature) and HadISST (for SST); (e–h) GISS. Black dots indicate statistical significance at the >95% confidence level, based on the *t*-test. Units: °C.

Han and Li 2016

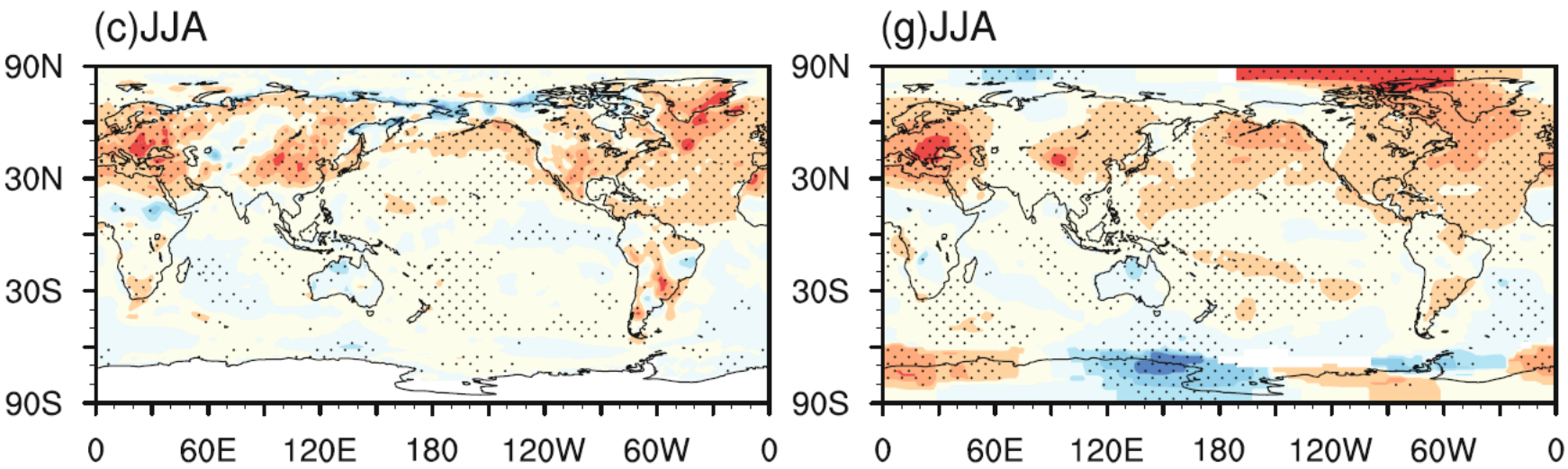
(c)JJA
90N
30N
30S
90S
0
60E
120E
180
120W
60W
0
(g)JJA
90N
30N
30S
90S
0
60E
120E
180
120W
60W
0

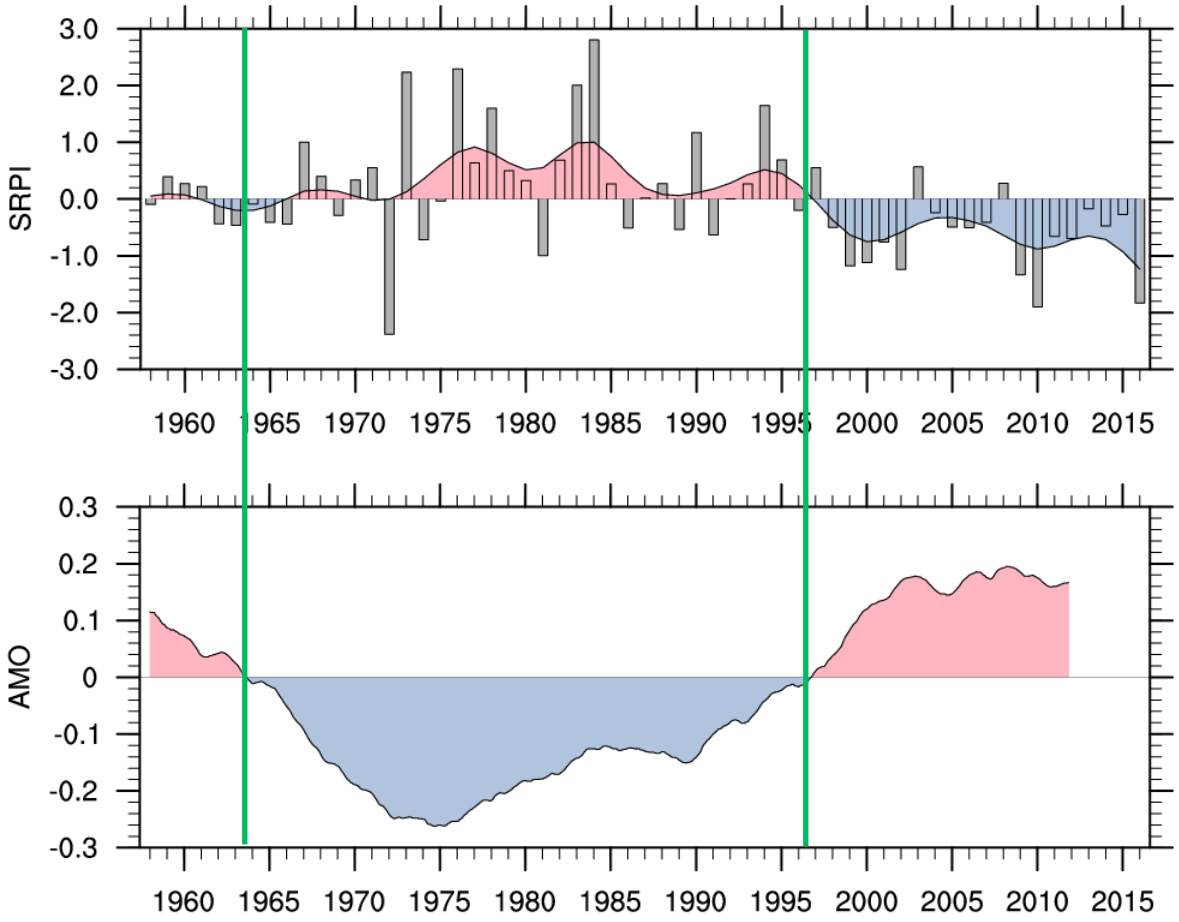

AMO concurs with the decadal change in SRP

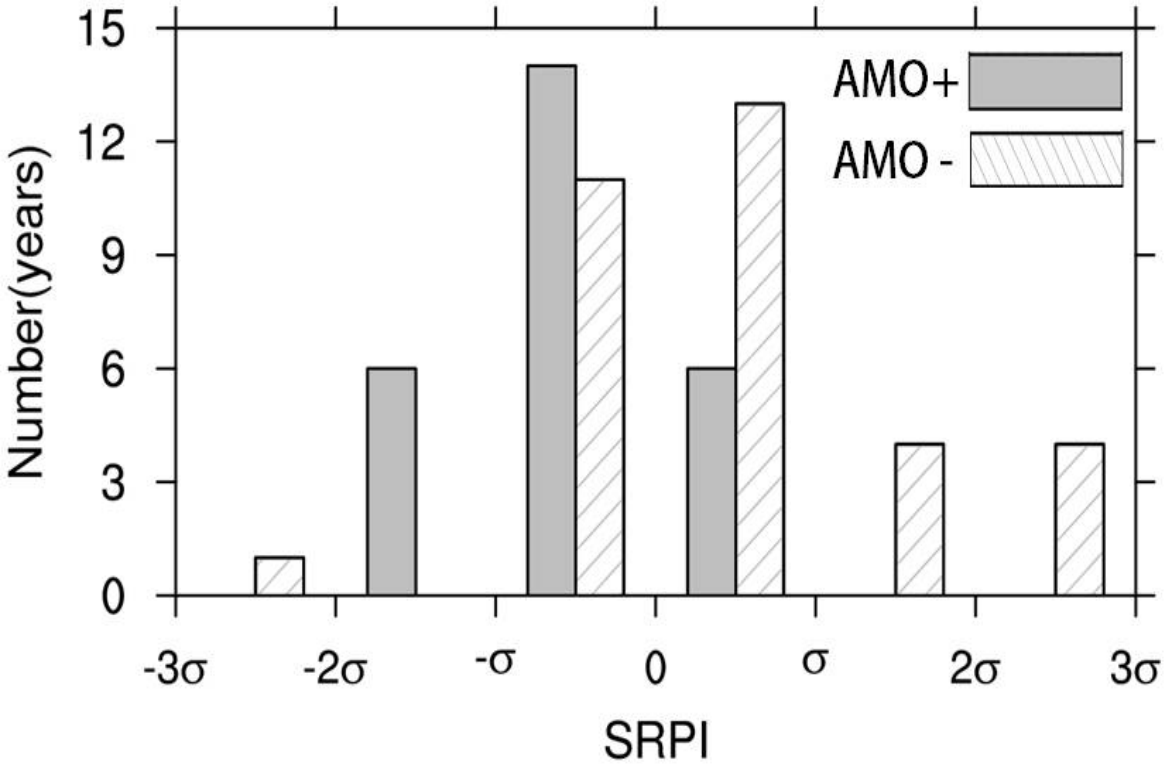
15
12
9
6
3
0
Number(years)
AMO+
AMO -
-3σ
-2σ
-σ
0
σ
2σ
3σ
SRPI

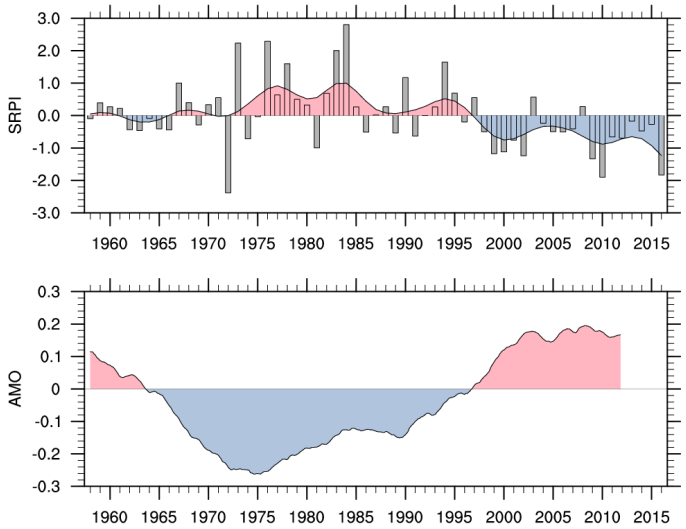
SRPI
3.0
2.0
1.0
0.0
-1.0
-2.0
-3.0
1960 1965 1970 1975 1980 1985 1990 1995 2000 2005 2010 2015
AMO
0.3
0.2
0.1
0
-0.1
-0.2
-0.3
1960 1965 1970 1975 1980 1985 1990 1995 2000 2005 2010 2015

We hypothesize that the AMO can affect circulations over Europe and then modulate the decadal change in SRP

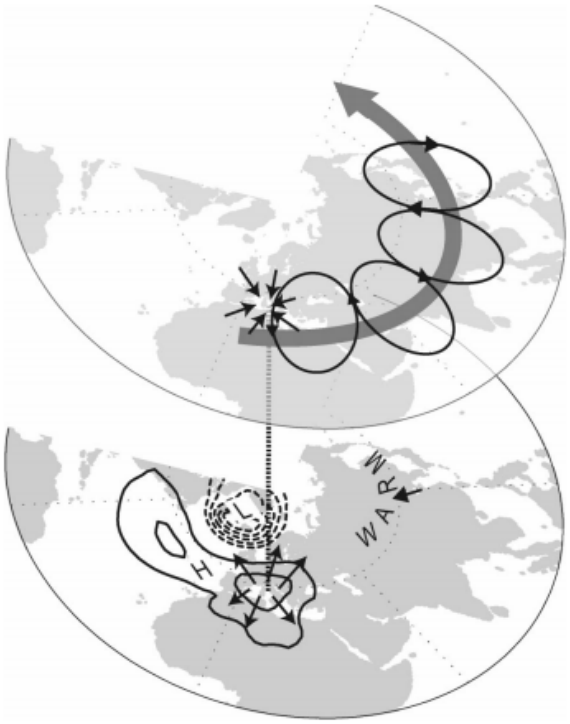

Watanabe 2004; Goswami et al. 2006

Summary

- The summer warming is amplified after the mid-1990s over Europe-West Asia and Northeast Asia.
- AMO induces this warming pattern by modulating the Silk Road Pattern—a dominant teleconnection pattern over the Eurasian continent in summer.
- The SRP exhibits a strong decadal variability, explaining about 30% of the total variance.

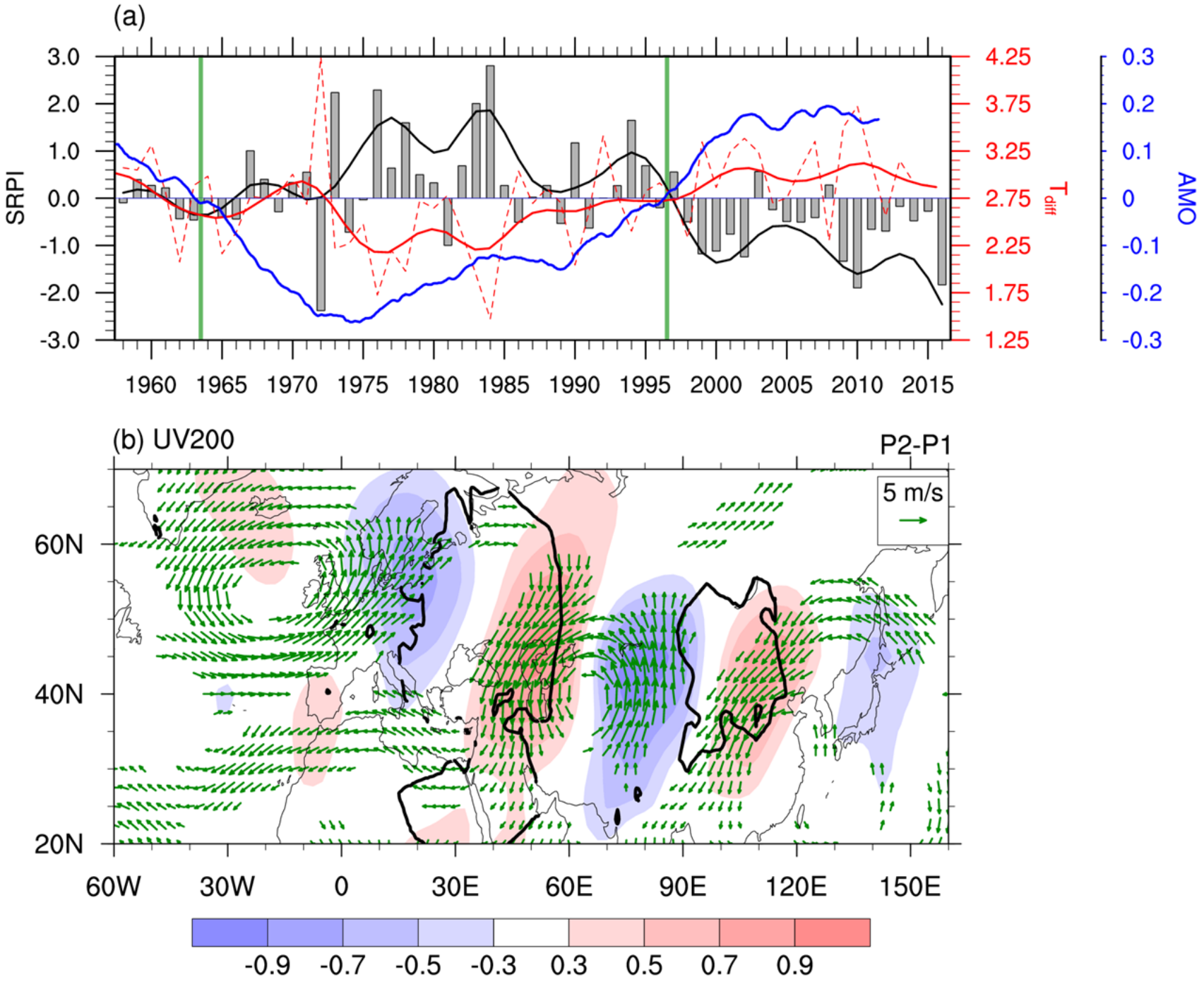
(a)
SRPI
3.0
2.0
1.0
0.0
-1.0
-2.0
-3.0
4.25
3.75
3.25
2.75
2.25
1.75
1.25
T diff
0.3
0.2
0.1
0
-0.1
-0.2
-0.3
AMO
1960 1965 1970 1975 1980 1985 1990 1995 2000 2005 2010 2015
(b) UV200
P2-P1
5 m/s
60N
40N
20N
60W 30W 0 30E 60E 90E 120E 150E
-0.9 -0.7 -0.5 -0.3 0.3 0.5 0.7 0.9